Research Article | Vol. 29, No. 16 / 2 August 2021 / Optics Express 25388
Optics EXPRESS

Localization-to-delocalization transition of light in frequency-tuned photonic moiré lattices

JIONGCHAO ZENG,[1] YANWEN HU,[1,2] XIN ZHANG,[1,2] SHENHE FU,[1,2,3,4] HAO YIN,[1,2,3] ZHEN LI,[1,2,3,5] AND ZHENQIANG CHEN[1,2,3]

[1]Department of Optoelectronic Engineering, Jinan University, Guangzhou 510632, China
[2]Guangdong Provincial Key Laboratory of Optical Fiber Sensing and Communications, Guangzhou 510632, China
[3]Guangdong Provincial Engineering Research Center of Crystal and Laser Technology, Guangzhou 510632, China
[4]fushenhe@jnu.edu.cn
[5]ailz286@126.com

Abstract: We demonstrate in a numerical manner the intriguing localization-to-delocalization transition of light in frequency-tuned photonic moiré lattices, both in the zero-order and the higher-order regimes of light waves. We present a different technique to realize the composite photonic lattices, by means of two relatively twisted sublattices with different modulated lattice constants. Even though various kinds of photonic patterns including the commensurable and the incommensurable lattices can be well constructed, the observed transition between the localization and the delocalization of light field is moiré angle-independent. This angle-insensitive property was not reported before, and cannot be achieved by those photonic moiré lattices that are all moiré angle-dependent. We reveal that the obtained phase transition of light is robust to the changes of refractive index modulation of the photonic lattices. Moreover, we reveal that the effect of moiré angle-independent transition of light can be extended to the higher-order vortex light field, hence allowing prediction, for the first time to our knowledge, of both the localization and the delocalization of the vortex light field in the photonic lattices.

1. Introduction

For a long time, it has been an important scientific and technological challenge to achieve localization of wave packets [1–4]. This is mainly because the wave is natively diffractive and dispersive during its propagation, leading to a broadening effect of wave. In order to overcome wave spreading, a common method is to use nonlinear response of optical materials [5,6]. For example, the induced nonlinear self-focusing effect tends to make the light wave converging, which balances the wave diffraction in the course of light propagation. As a result, the wave evolves in a form of solitary mode which does not change its shape during propagation [5]. This common technique was exploited extensively to arrest the diffraction/dispersion in many different types of physical settings, e.g., see relevant references among them [7–13]. Note that this nonlinear method requires a very strong intensity of wave to induce sufficient change of the refractive index in the medium, since the nonlinear coefficient is usually very small [6]. This would be undesirable and significantly increase the challenge in reality.

Recently, moiré lattice has been demonstrated as an effective linear way to overcome the diffraction of waves [14–17], hence giving rise to localization of the wave when it propagates through the moiré lattice. The moiré lattice can be realized by combining two identical periodic lattices with a relatively rotation angle between them [14]. The resultant moiré structure exhibits a supercell that strongly relies on the moiré angle. Recent studies suggest that by carefully twisting the moiré angle of the lattices, one can obtain various patterns for the photonic moiré lattices,

#434281 https://doi.org/10.1364/OE.434281
Journal © 2021 Received 16 Jun 2021; revised 16 Jul 2021; accepted 19 Jul 2021; published 23 Jul 2021

Optics EXPRESS

including the periodic and the aperiodic (quasiperiodic) structures [14–16]. Using these moiré lattices, both the localization and delocalization of light waves can be observed [15]. Note that these moiré lattices can be realized either by the technique of direct femtosecond laser writing or optical induction with a photorefractive crystal [18,19]. It is important to note that solitary modes of wave forms can be also achieved in the moiré lattices with nonlinear response, in which case the power/intensity threshold for nonlinear excitation of the solitary waves is significantly reduced [16].

The underlying physics for localizations of the wave packets in the moiré lattices is that they exhibit many fundamental flat-band structures in the Fourier space [14–16]. A flat band indicates a nondispersive energy band where a localized state of light can be supported. This resembles phenomenon appearing in the bilayer structures with a twisting moiré angle between them [20–23], as demonstrated earlier than the photonic moiré lattices. These bilayer structures exhibit analogous flat-band structures where the electron becomes localized at the compact flat band and exhibits no motion inside the structure. Therefore, the moiré lattice can be potentially considered as a useful device in the field of information processing [20–23]. It also offers a powerful platform to manipulate propagation dynamics of the light beams [14–17].

Nevertheless, the recent interest in light localization and delocalization in moiré photonic lattices brings about the following intriguing questions. Firstly, the common method to construct the moiré lattices, so far, is based on twisting the two identical periodic lattices [14–16]. An interesting question is whether there is moiré photonic lattice which is insensitive to the moiré angle, while it also exhibits clear localization-delocalization transition of light. Secondly, can the moiré lattices support localization for the higher-order topological light waves, e.g., the wave featured by a vortex-phase wave front? These issues were not addressed before, neither in theory nor in experiment. But they are appearing for fundamental understandings in this particular hot topic of the moiré photonic lattices which has already attracted wide attention recently [17,24–28]. In this work, we address these issues, presenting a different technique to construct the moiré lattice that is insensitive to the moiré angle. Owing to its immunity to the moiré angle, the transition between the localization and delocalization of the wave packets is possible, both for the commensurable and the incommensurable moiré lattices.

2. Theoretical model

In this work, we introduce a different technique for constructing a frequency-tuned moiré lattice, by mean of two periodic sublattices which have different spatial modulation frequencies (i.e., their lattice constants are slightly mismatched), and are twisted relatively. We express the resultant photonic lattice in a form of

$$V = V_1(x,\ y) + V_2(x',\ y'), \tag{1}$$

where V_1=cos(f_1x)+cos(f_1y), and V_2=cos(f_2x')+cos(f_2y') denote two square photonic sublattices, respectively, with f_1 and f_2 being their spatial modulation frequencies. x and y are the transverse coordinates. Note that these two sublattices have the same intensity contrast and are twisted with a relative moiré angle of θ, associated with the rotational matrix $R(\theta)$=[cos(θ), -sin(θ); sin(θ), cos(θ)]. In this regard, the sublattice V_2 is represented in a rotated coordinate system x' and y', expressed as (x'; y')= R(θ)*(x; y). It is suggested that the resultant form of the lattice pattern strongly depends on the choice of modulation frequencies. Typical examples of the twisted photonic lattices are simulated based on the formula in Eq. (1), with outcomes illustrated in Fig. 1. In simulations, we set the modulation frequencies of the two sublattices as f_1=2000 cm^{-1} and f_2=af_1 where a is a mismatched coefficient to the sublattice V_1. It is clearly seen from Fig. 1 that both the commensurable and the incommensurable photonic lattices can be well constructed by slightly tunning the mismatch factor a.

To illustrate these patterns, we firstly consider the commensurable lattices with the help of the Pythagorean theorem [14]. We present the Pythagorean triples as (c_1, c_2, c_3), satisfying

Optics EXPRESS

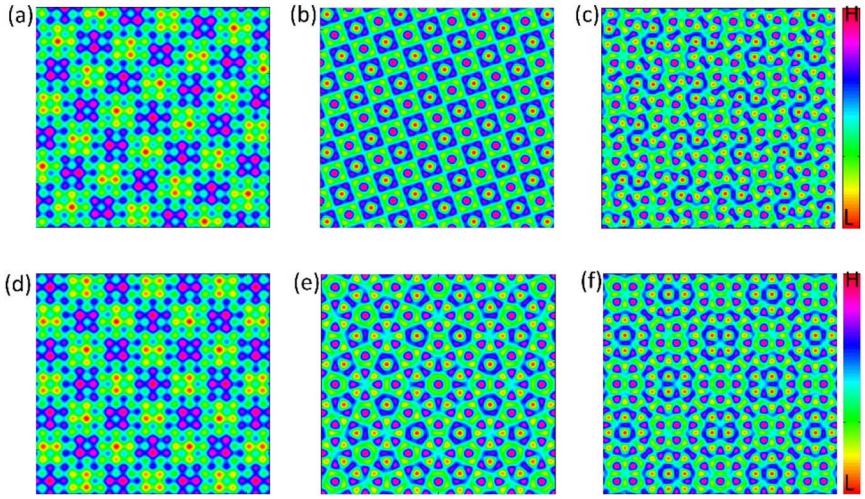

Fig. 1. Composite photonic lattices constructed by two periodic square sublattices with different mismatched factors: (a)(d) a = 0.3; (b)(e) a = 1.0; and (c)(f) a = 1.2. The twisting angle between the two sublattices is set as: (a)-(c) θ = atan(3/4) (the commensurable angle), and (d)-(f) $\theta = \pi/4$ (the incommensurable angle). These patterns are obtained based on the Eq. (1). All the panels share the same scale. In the color bars, L: Low; H: High.

the relationship: $c_1{}^2+c_2{}^2=c_3{}^2$. Based on the Pythagorean theorem, we can obtain a series of Pythagorean triples, including (3, 4, 5) and (5, 12, 13), and so on. By setting the moiré angle that satisfies θ=atan(3/4) or θ=atan(5/12), we can obtain the typical commensurable lattices, e.g., see the one in Fig. 1(b) for the Pythagorean triples (3, 4, 5), in the case of a=1. The resultant photonic lattice exhibits clear periodicity with the same lattice constant to the sublattices. Owing to the moiré rotation of the two sublattices, the obtained periodic lattice has a relatively twist with respect to the untwisted sublattices. The commensurable lattices degrade into the incommensurable ones when decreasing and increasing the mismatch factor a, see the corresponding results in Figs. 1(a) and 1(c), for the cases of a=0.3 and a=1.2, respectively. These results indicate that the mismatched photonic lattices are aperiodic, but exhibit intriguing rotational symmetry in the Fourier space, which can be identified from their corresponding Fraunhofer diffraction patterns in the far field, as illustrated in Figs. 2(a) and 2(c), respectively. Note that these diffraction patterns can be generated by Fourier transform of the lattice patterns shown by Eq. (1).

Figures 2(a)–2(c) show a transition between the aperiodic and periodic photonic lattices. Figures 2(a) and 2(c) demonstrate a four-fold rotational symmetry of the diffraction patterns, indicating the aperiodic structures as depicted in Figs. 1(a) and 1(c), respectively; whereas for a matched lattice (a=1.0), the corresponding far-field diffraction of the lattice exhibits regular pattern, as shown in Fig. 2(b). It is suggested from these results that in the cases of the mismatched lattices, a change of the modulation frequency does not affect the four-fold symmetric property of the moiré latices. It means that one can slowly tune the modulation frequencies of the sublattices to obtain a series of moiré lattices having the same rotational symmetry, and to see the underlying phase transition, which appears in the vicinity of the matched lattices (a=1.0). This feature can be also seen from another moiré angle, e.g., see the lattice patterns in Figs. 1(d)–1(f), for a typical incommensurable angle of θ=π/4. In this case, the mutual interference of the two sublattices leads to the incommensurable photonic moiré lattices. Similarly, the mismatched lattices (a≠1.0) exhibits the same four-fold rotational symmetry to the commensurable cases, as illustrated by their Fraunhofer diffraction patterns in Figs. 2(d) and 2(f), respectively. However, for the matched

Optics EXPRESS

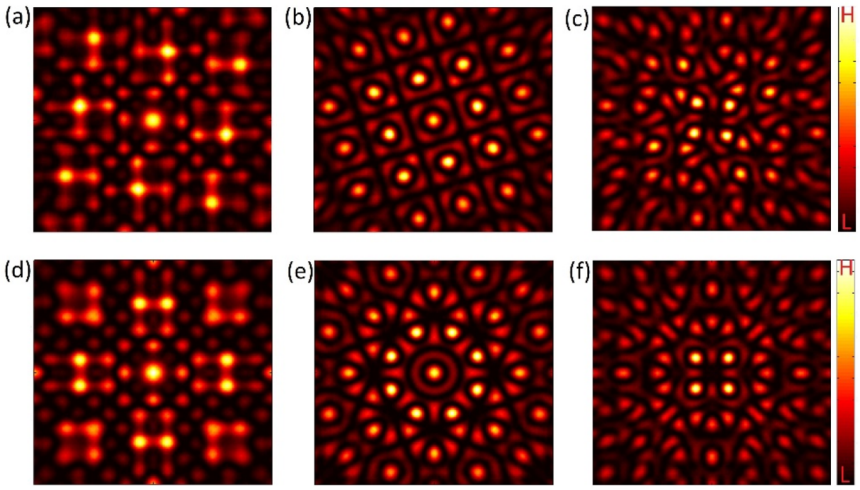

Fig. 2. The corresponding Fraunhofer diffraction patterns of the photonic moiré lattices shown in Fig. (1). Parameters for the photonic lattices are specified as: (a)(d) $a = 0.3$; (b)(e) $a = 1.0$; and (c)(f) $a = 1.2$. The twisting angle between the two sublattices is set as: (a)-(c) $\theta = \text{atan}(3/4)$, and (d)-(f) $\theta = \pi/4$. These panels have the same scale.

lattice (a=1.0), see Fig. 1(e) as well as its Fourier pattern in Fig. 2(e), it exhibits a different 8-fold rotational symmetry. This is a critical transition point (a=1.0) among the moiré lattices. Our simulations suggest that both the commensurable and the incommensurable moiré lattices exhibit phase transition appearing in the vicinity of a=1.0.

The proposed scheme for creating the moiré structure is tunable, which leads to creation of photonic lattices with controllable shapes and sizes. In the following, we expect that the localization-delocalization transition would be revealed by these frequency-tuned photonic moiré lattices, owing to the critical phase transition of the lattice structures at the matched condition (a=1.0). Propagation dynamics of a light wave along z axis in the moiré photonic lattices can be described by the paraxial Schrödinger-like wave equation, written as [29,30]

$$i\frac{\partial E(x,y,z)}{\partial z} + \frac{1}{2n_0k_0}\nabla^2 E(x,y,z) + k_0\Delta n(x,y)E(x,y,z) = 0 \tag{2}$$

where $E(x, y, z)$ denotes the envelope field slowly varying with the propagation distance z, and $k_0 = 2\pi/\lambda$ is the carrier wave number in the vacuum, with λ being the optical wavelength. Here $\nabla^2 = \partial_x^2 + \partial_y^2$ represents transverse Laplacian operator. n_0 denotes the refractive index of a bulk material, while $\Delta n(x, y) = dn \cdot V(x, y)$ represents the refractive index distribution of the photonic lattices induced optically in the bulk material, where dn denotes the modulation depth of the refractive index. Thus, the value of $\Delta n(x, y)$ fluctuates at the bulk (average) index n_0. The photonic lattice we studied here is a two-dimensional system, with both the periodic and aperiodic (quasiperiodic) fluctuation of the refractive index in the transverse plane, while it is independent on the propagation distance z. This is different from two-dimensional dynamical quasicrystals [31], which involves with dynamical behaviors. But their stationary patterns exhibit similar quasiperiodic structures to those considered in this work. The similarity can be seen from their high rotational symmetry of the patterns, e.g., the eight-fold quasiperiodic pattern [see Fig. 2(e)].

Equation (2) is tantamount to the Schrödinger equation for the quantum mechanics. Thus, the broadening effect can be arrested by putting the wave into an effective potential, in a manner similar to a quantum particle that is trapped by the potential well [32]. Therefore, the refractive

Optics EXPRESS

index distribution $\Delta n(x, y)$ plays a role as an effective quasi-periodic potential for trapping the light fields. Such a quasi-periodic potential is related to the transverse distribution of the refractive index, where the modulation depth characterizes the potential depth. Indeed, intriguing wave phenomena including Bloch oscillations [33,34], dynamic localizations [35], and optical tunnelling [36] were revealed by properly engineering $\Delta n(x, y)$. Here we design the tunable moiré photonic lattices, to reveal the underlying localization-to-delocalization transition of light. To this end, we send a Gaussian beam as a probe beam into the lattice. In this scenario, the initial condition for the wave equation in Eq. (2) can be expressed as

$$E(x, y, z = 0) = E_0 \exp\left(-\frac{x^2 + y^2}{\sigma^2}\right) \tag{3}$$

where E_0 is the incident amplitude of the probe beam, and σ is the Gaussian duration. In the following, we utilize the model shown in Eq. (2), together with the initial condition in Eq. (3), to demonstrate numerically the underlying phenomena of light localization and delocalization. We finally modify the initial condition, by adding a complex phase profile, to investigate how the photonic lattices affect propagation dynamics of a higher-order topological field.

3. Results and discussions

We simulate propagation dynamics of the probe beam described by the Eq. (3) in the photonic moiré lattices, based on the paraxial Schrödinger-like wave equation in Eq. (2). The linear wave equation can be numerically solved with the help of the fast-Fourier-transform algorithm. In simulations, we set the carrier wavelength of $\lambda = 632.8$ nm, and consider the photonic lattices (f_1=2000 cm^{-1}) presented in the Fig. 1, with a refractive index contrast of $dn = 5 \times 10^{-5}$ induced in the bulk material (n_0=2.0). Note that our methodology for observation of localization-to-delocalization transition of light is independent of n_0, not limited to the case used here. A Gaussian probe beam with a diameter of $\sigma = 10$ μm is launched at the center position of the lattices. Figure 3 illustrates the corresponding output results of the light after propagation through the photonic lattices with interaction length of z=25 mm. First, let us see the results depicted in Figs. 3(a) and 3(d) with the mismatched photonic lattices (a=0.3) both for the commensurable and the incommensurable moiré angles. It is clearly observed that the probe light can be highly localized during propagation in these two lattices. The light localization can be further emphasized by a comparison to the free-space propagation of light having the same initial Gaussian waist, in which case the Rayleigh range of the fee-space propagating light is estimated as $z_R = \pi\sigma^2/\lambda = 0.5\ mm$, much smaller than the propagation length of the beam in the lattices. However, the light becomes weakly localized in the matched lattices (a=1.0) under the same conditions. This can be demonstrated from Figs. 3(b) and 3(e) for the two moiré angles, showing significant side lobes around the central main lobes. Figures 3(b) and 3(e) further reveal that the incommensurable lattices support relatively more localized wave packet than the commensurable one, at the same condition. This is because the incommensurable angle corresponds to aperiodic lattice that could support flat-band state of light, which propagates in the lattices with weak diffraction; whereas the periodic lattices do not exhibit this intriguing nondiffracting property. By slightly increasing the mismatch factor to a=1.2, it is intriguing to find that, although the resultant photonic lattices are aperiodic, the light becomes completely delocalized as indicated from their corresponding output intensity distributions in Figs. 3(c) and 3(f), respectively. From these results, it is evident that localization and delocalization of light can be controlled and tuned by the mismatched factor a.

Importantly, it is further indicated that the frequency-tuned photonic lattice is insensitive to the moiré angle, which is different from the extensively studied angle-sensitive moiré lattices [14–16]. In the cases we discussed here, both the commensurable and incommensurable lattices exhibit similar localization-to-delocalization transition of light, as observed from the light patterns in

Optics EXPRESS

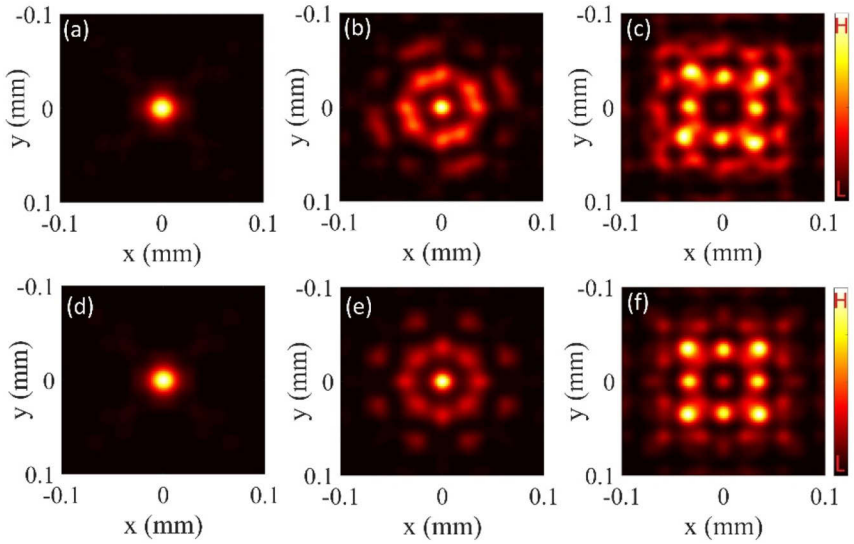

Fig. 3. Demonstration of localization and delocalization of light fields. Intensity distributions of the light fields after passing thought the photonic lattices (z=25 mm) are presented. The parameters for the photonic lattices are specified as: (a)(d) $a = 0.3$; (b)(e) $a = 1.0$; and (c)(f) $a = 1.2$. The twisting angle between the two sublattices is set as: (a)-(c) $\theta = \text{atan}(3/4)$, and (d)-(f) $\theta = \pi/4$. These simulated results were obtained based on Eqs. (2) and (3).

Fig. 3. Also, it was already shown that the commensurable lattices do not support localized wave packets [15]. This is not true for the mismatched photonic lattices, as we demonstrated in Fig. 3(a). We present state transition of light by tuning the spatial frequencies of the sublattices, regardless of the moiré angles we used here.

We further examine the transition between localization and delocalization of light by scanning the mismatched factor within an interval. To this end, we introduce a form factor to characterize the spatial confinement of light field in the photonic lattices. We express the form factor as [29]

$$w = \frac{\left(\iint |E(x,y)|^4 dxdy\right)^{1/2}}{\iint |E(x,y)|^2 dxdy} \tag{4}$$

Note that w is inversely propagational to the spatial size of the light field, i.e., the larger value of w corresponds to a more localized wave packet that is trapped in the photonic lattices. By investigating how the form factor w of the wave develops with gradually scanning the mismatched factor, we can identify directly the phase transition of the light mode from localization to delocalization in the lattices. Therefore, we simulate the dependency of w on the mismatched factor a, with outcomes presented by the blue curves in Figs. 4(a) and 4(b), for both the commensurable and the incommensurable moiré lattices, respectively. It is evident that with the increasing of a, the value of w at the beginning is very strong ($w \cong 200$) and remains approximately unchanged. At this regime, phenomenon of light localization can be observed significantly. Afterwards, it starts to decline sharply when a approaching the value of 1. It reaches its minimum ($w \cong 50$) and becomes nearly invariant when a exceeds 1, as seen from the blue curves in Figs. 4(a) and 4(d). This significant decrease of w indicates a clear transition from localization to delocalization of light near the critical value of a=1. We further confirm these assertions by presenting the light field distributions at the value of a=0.9 and a=1.1, after a propagation distance of z=25 mm, see the results in Figs. 4(b), 4(c) and Figs. 4(e), 4(f), for the two

Optics EXPRESS

typical moiré angles, respectively. For both cases, the light is localized at a=0.9, but it becomes delocalized at a=1.1, showing a sharp transition between two different light modes. Besides, we note that the value of w in both the considered moiré angles share similar dependencies on a, further suggesting that the design photonic lattice is insensitive to the moiré angle.

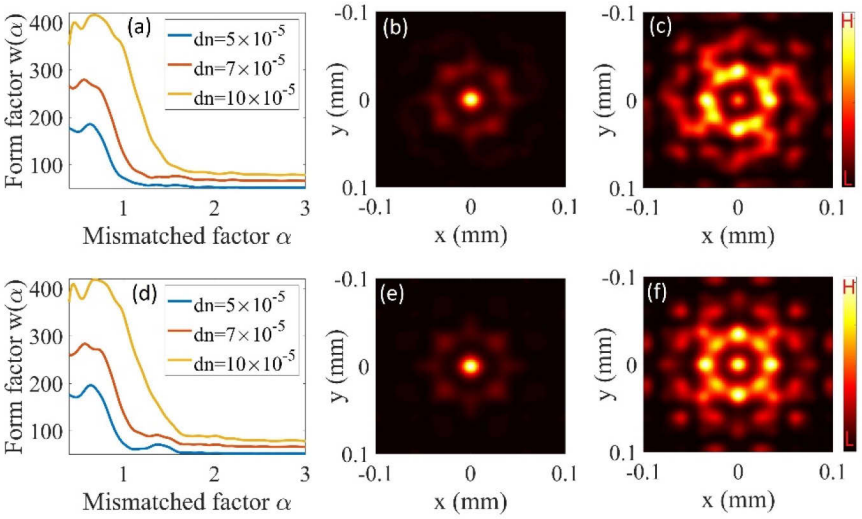

Fig. 4. Demonstration of localization-to-delocalization transition of light field. (a)(d) Form factor as a function of mismatched factor, for two cases: (a) θ = atan(3/4), and (d) $\theta = \pi/4$. (b)(c) and (e)(f) show intensity distributions of the light fields after passing thought the lattices with interaction length of z=25 mm, under the settings: (b)(c) θ = atan(3/4), and (e)(f) $\theta = \pi/4$; (b)(e) a = 0.9, and (c)(f) a = 1.1. These results were obtained based on Eqs. (2) and (3).

We examine the influences of the modulation depth of refractive index of the photonic lattices on the light localization and delocalization. This is important since the photonic lattice actually acts as an effective potential that can trap or diffuse light during its propagation. The larger modulation of the refractive index indicating a stronger effective potential. As a result, the light would be more easily to be localized during evolution in the photonic lattices. This effect can be also observed from the dependence curves of w on a, as shown in Figs. 4(a) and 4(d) for both two moiré angles. As expected, the value of the form factor w, indeed, becomes relatively stronger with a larger modulation depth dn. In this case, it is relevant to mention that what makes light localized is not only the moiré structures, but also the refractive index of the lattice itself that comes into play a role on the localization of the light wave. To illustrate this point more specifically, we present the intensity distributions of the light fields after a propagation distance of z=25 mm, see the outcomes in Fig. 5. Figures 5(a) and 5(d) show the localized modes supported both by the commensurable and incommensurable lattices at the mismatched factor of a=0.5. Owing to a larger value of dn, the regime for the localized modes can be extended beyond a=1.0, as seen from the dependency of w on a. Compared to the results shown in Figs. 3(b) and 3(e), the results shown in Figs. 5(b) and 5(e) demonstrate a more localized light modes at the critical value of a=1.0. When a exceeds its critical point, the mode profile becomes significant larger, corresponding to a delocalized mode, e.g., see the outcome in Figs. 5(c) and 5(f) for the case of a=2.0. Moreover, it is worth mentioning that the localization-to-delocalization transition appears in the vicinity of a=1.0, for all these cases of modulation depth of the refractive index. This intriguing independent transition on the refractive index modulation, as well as on the moiré angle, was not reported up to this work.

Optics EXPRESS

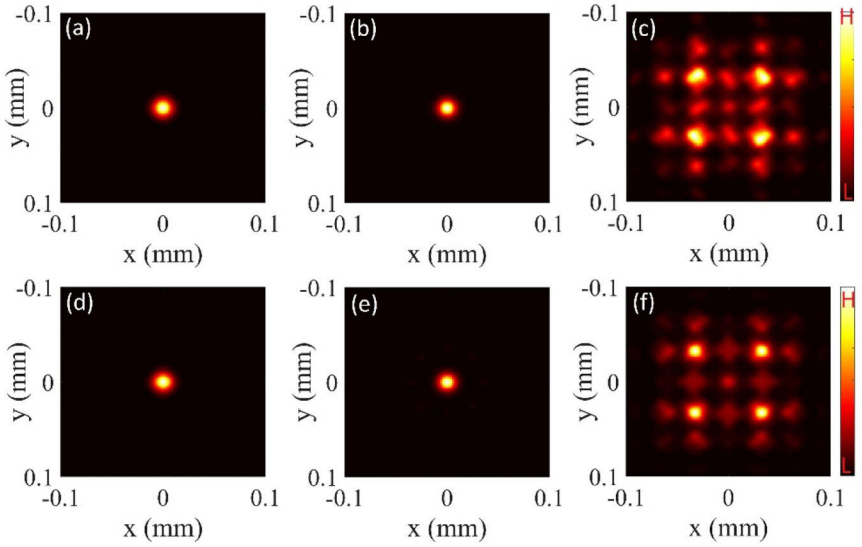

Fig. 5. Localization and delocalization of light fields with a larger modulation depth $dn = 10 \times 10^{-5}$. It shows intensity distributions of the fields at z=25 mm. Parameters for the lattices are specified as: (a)(d) $a = 0.5$; (b)(e) $a = 1.0$; and (c)(f) $a = 2.0$. The twisting angle between the two sublattices is set as: (a)-(c) $\theta = \text{atan}(3/4)$, and (d)-(f) $\theta = \pi/4$.

Finally, we are interested in the investigations of the localization-to-delocalization transition of a higher-order topological vortex field in the photonic moiré lattices. The vortex light field exhibits a space-variant phase profile, characterized by a topological number l. The vortex beam has been attracting significant attention owing to its great interest in both the fundamental and the applicable studies [37,38]. Notwithstanding progress of the vortex light field, whether the moiré lattices could support localization-to-delocalization transition for the higher-order topological fields remain unknown, to our knowledge. To examine this higher-order transition, we modify the initial condition as

$$E(x, y, z = 0) = E_0 r \exp\left(-\frac{r^2}{\sigma^2}\right) \exp(il\varphi) \tag{5}$$

where $r = \sqrt{x^2 + y^2}$, and $\varphi = \arctan(y/x)$ denote, respectively, the radial distance and azimuthal angle in the polar coordinates. Equation (5) indicates that the incident light field has a Laguerre-Gauss profile, coupled by the vortex phase. Hence, its intensity features by a doughnut shape in the transverse plane. Note that owing to the vortex phase profile, this structured light field exhibits more seriously diffraction than the zero-order Gaussian field described by the Eq. (3), in the course of their propagations. Despite of this effect, we still reveal that the vortex field can also be localized in the photonic moiré lattices.

Let's firstly consider a photonic lattice with a typical moiré angle of $\theta = \pi/4$, and a mismatched factor of a=0.4. With these settings, simulations are carried out for the first-order (l=1) vortex light field, based on the initial condition in Eq. (5). It is shown from Fig. 6(a) that a localized light field having the doughnut shape in the transverse plane is obtained, indicating a localized higher-order light mode. Additionally, the topological phase structure of the localized light mode is found to be preserved when it passes through the photonic lattice, as illustrated in Fig. 6(d). For another case of the photonic lattice at the transition point a=1.0, a relatively weak localized mode can still be observed, as suggested by the approximate ring pattern in Fig. 6(b), as well as its corresponding phase structure in Fig. 6(e). In this case, in addition to the central main ring, there are certain side lobes in the pattern, indicating a weakly diffusing effect in the lattice. However,

Optics EXPRESS

for a larger value of mismatched factor (a=1.2), the localized vortex mode becomes delocalized, as adjusted from the resultant pattern in Fig. 6(c). In this case, the interaction between the vortex field and the photonic lattice leads to many phase singularities having the same topological charge of $|l|$=1, but distributed at different positions as shown in Fig. 6(f). This is a manifestation of the diffusion effect of the vortex light in the lattice. From these results, we can see that both the localization and delocalization can be observed by tuning the mismatched factor of the lattice. Therefore, such localization-to-delocalization transition still can be identified in the higher-order regime of light waves.

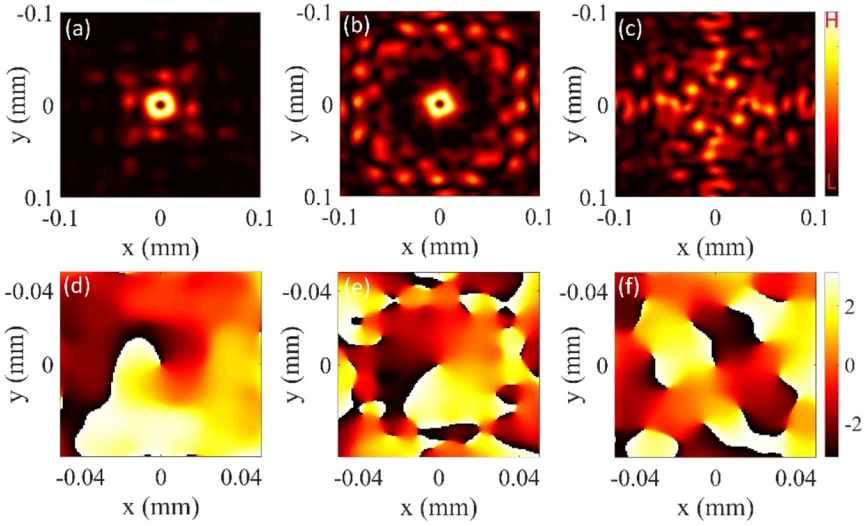

Fig. 6. Localization and delocalization of the higher-order vortex light fields (l=1). (a)-(c) Intensity distributions of the light fields after passing thought the photonic lattices with interaction length of z=25 mm. The parameters for the photonic lattices are specified as: (a) a = 0.4; (b) a = 1.0; and (c) a = 1.2. The twisting angle for the lattices is set as $\theta = \pi/4$. (d)-(f) Corresponding phase profiles of (a)-(c). Simulations were based on Eqs. (2) and (5).

4. Conclusion

In summary, we have demonstrated numerically the localization-to-delocalization transition of light in frequency-tuned photonic moiré lattices. We introduced a different technique to construct the photonic moiré lattices, by means of two twisted square sublattices with different lattice constants (we have recently found that moiré photonic patterns can also be generated without physical rotations [39]). The relatively twisting between the two sublattices, together with their tunable lattice constants, allows creation of many different lattice patterns, including the commensurable and the incommensurable photonic moiré lattices. However, our results reveal that the resultant frequency-tuned photonic lattice is moiré angle-insensitive, hence enables observation of the moiré angle-independent phase transition of the light mode. Our demonstration is connected to the Anderson localization in a quasiperiodic potential [40,41], where a transition from delocalized to localized Bose-Einstein condensate state was displayed, analogous to state transition of light reported in our work. But this work contrasts to previous schemes based on quasicrystals where disorder is required for Anderson localization [42].

We have investigated the influences of the modulation depth of the refractive index of the photonic lattices. It is interesting to find that the localization-to-delocalization transition appears in the vicinity of a=1.0, for all the considered cases of modulation depth of the refractive index.

Optics EXPRESS

Importantly, we have shown that the moiré angle-independent transition of light can be extended to the higher-order regime of waves, where we have examined the localization and delocalization of vortex light field in the photonic lattices. This higher-order effect was not reported before, to the best of our knowledge. This demonstration opens a new avenue to manipulate the state of light in the photonic lattices, both in the zero-order and the higher-order regimes. Our demonstration may also trigger potential studies of other waves that satisfy the Schrödinger-like wave equation, including the waves in Bose-Einstein condensates [40,41,43].

Funding. Guangzhou Municipal Science and Technology Project (201904010094); National Natural Science Foundation of China (11974146); Special Project for Research and Development in Key areas of Guangdong Province (2020B090922006); Science and Technology Planning Project of Guangdong Province (2018B010114002); Guangdong Provincial Pearl River Talents Program (2017GC010280).

Disclosures. The authors declare no conflicts of interest.

Data availability. Data underlying the results presented in this paper are not publicly available at this time but may be obtained from the authors upon reasonable request.

References

1. F. Lederer, G. I. Stegeman, D. N. Christodoulides, G. Assanto, M. Segev, and Y. Silberberg, "Discrete solitons in optics," Phys. Rep. **463**(1-3), 1–126 (2008).
2. A. Chong, W. H. Renninger, D. N. Christodoulides, and F. W. Wise, "Airy-Bessel wave packets as versatile linear light bullets," Nat. Photonics **4**(2), 103–106 (2010).
3. S. Fu, Y. Tsur, J. Zhou, L. Shemer, and A. Arie, "Propagation Dynamics of Nonspreading Cosine-Gauss Water-Wave Pulses," Phys. Rev. Lett. **115**(25), 254501 (2015).
4. S. Fu, Y. Tsur, J. Zhou, L. Shemer, and A. Arie, "Propagation Dynamics of Airy Water-Wave Pulses," Phys. Rev. Lett. **115**(3), 034501 (2015).
5. Y. V. Kartashov, B. A. Malomed, and L. Torner, "Solitons in nonlinear lattices," Rev. Mod. Phys. **83**(1), 247–305 (2011).
6. L. Song, S. Fu, Y. Liu, J. Zhou, V. G. Chigrinov, and I. C. Khoo, "Direct femtosecond pulse compression with miniature-sized Bragg cholesteric liquid crystal," Opt. Lett. **38**(23), 5040–5042 (2013).
7. Y. Liu, H. Liang, C. Chen, X. Xie, W. Hu, P. Chen, J. Wen, J. Zhou, T. Lin, and I. C. Khoo, "Ultrafast switching of optical singularity eigenstates with compact integrable liquid crystal structures," Opt. Express **26**(22), 28818–28826 (2018).
8. S. Fu, Y. Liu, Y. Li, L. Song, J. Li, B. A. Malomed, and J. Zhou, "Buffering and trapping ultrashort optical pulses in concatenated Bragg gratings," Opt. Express **38**(23), 5047–5050 (2013).
9. M. Peccianti, K. A. Brzdakiewicz, and G. Assanto, "Nonlocal spatial soliton interactions in nematic liquid crystals," Opt. Lett. **27**(16), 1460–1462 (2002).
10. J. Safioui, F. Devaux, and M. Chauvet, "Pyroliton: pyroelectric spatial soliton," Opt. Express **17**(24), 22209–22216 (2009).
11. A. Chabchoub, O. Kimmoun, H. Branger, N. Hoffmann, D. Proment, M. Onorato, and N. Akhmediev, "Experimental Observation of Dark Solitons on the Surface of Water," Phys. Rev. Lett. **110**(12), 124101 (2013).
12. L. Shemer and B. Dorfman, "Experimental and numerical study of spatial and temporal evolution of nonlinear wave groups," Nonlin. Processes Geophys. **15**(6), 931–942 (2008).
13. X. Zhang, X. Xu, Y. Zheng, Z. Chen, B. Liu, C. Huang, B. A. Malomed, and Y. Li, "Semidiscrete quantum droplets and vortices," Phys. Rev. Lett. **123**(13), 133901 (2019).
14. C. Huang, F. Ye, X. Chen, Y. V. Kartashov, V. V. Konotop, and L. Torner, "Localization-delocalization wavepacket transition in Pythagorean aperiodic potentials," Sci. Rep. **6**(1), 32546 (2016).
15. P. Wang, Y. Zheng, X. Chen, C. Huang, Y. V. Kartashov, L. Torner, V. V. Konotop, and F. Ye, "Localization and delocalization of light in photonic moiré lattices," Nature **577**(7788), 42–46 (2020).
16. Q. Fu, P. Wang, C. Huang, Y. V. Kartashov, L. Torner, V. V. Konotop, and F. Ye, "Optical soliton formation controlled by angle twisting in photonic moiré lattices," Nat. Photonics **14**(11), 663–668 (2020).
17. B. Lou, N. Zhao, M. Minkov, C. Guo, M. Orenstein, and S. Fan, "Theory for Twisted Bilayer Photonic Crystal Slabs," Phys. Rev. Lett. **126**(13), 136101 (2021).
18. S. Xia, D. Song, N. Wang, X. Liu, J. Ma, L. Tang, H. Buljan, and Z. Chen, "Topological phenomena demonstrated in photorefractive photonic lattices," Opt. Mater. Express **11**(4), 1292–1312 (2021).
19. J. Lyu, Z. Wen, K. Han, X. Qi, and Y. Gao, "Nonlinear transmission and pseudospin in two-dimensional octagon and dodecagon photonic lattices," Opt. Mater. Express **8**(9), 2713–2721 (2018).
20. C. R. Woods, L. Britnell, A. Eckmann, R. S. Ma, J. C. Lu, H. M. Guo, X. Lin, G. L. Yu, Y. Cao, R. V. Gorbachev, A. V. Kretinin, J. Park, L. A. Ponomarenko, M. I. Katsnelson, Y. N. Gornostyrev, K. Watanabe, T. Taniguchi, C. Casiraghi, H.-J. Gao, A. K. Geim, and K. S. Novoselov, "Commensurate-incommensurate transition in graphene on hexagonal boron nitride," Nat. Phys. **10**(6), 451–456 (2014).

Optics EXPRESS

21. Y. Cao, J. Y. Luo, V. Fatemi, S. Fang, J. D. Sanchez-Yamagishi, K. Watanabe, T. Taniguchi, E. Kaxiras, and P. Jarillo-Herrero, "Superlattice-Induced Insulating States and Valley-Protected Orbits in Twisted Bilayer Graphene," Phys. Rev. Lett. **117**(11), 116804 (2016).
22. N. N. T. Nam and M. Koshino, "Lattice relaxation and energy band modulation in twisted bilayer graphene," Phys. Rev. B **96**(7), 075311 (2017).
23. Y. Cao, V. Fatemi, A. Demir, S. Fang, S. L. Tomarken, J. Y. Luo, J. D. Sanchez-Yamagishi, K. Watanaber, T. Taniguchi, E. Kaxiras, R. C. Ashoori, and P. Jarillo-Herrero, "Correlated insulator behaviour at half-filling in magic-angle graphene superlattices," Nature **556**(7699), 80–84 (2018).
24. Q. Zhang, Q. Qu, G. Hu, J. Liu, Z. Dai, M. S. Fuhrer, Q. Bao, and C. Qiu, "Hybridized Hyperbolic Surface Phonon Polaritons at α-MoO_3 and Polar Dielectric Interfaces," Nano Lett. **21**(7), 3112–3119 (2021).
25. G. Hu, C. Zheng, J. Ni, C. Qiu, and A. Alù, "Enhanced light-matter interactions at photonic magic-angle topological transitions," Appl. Phys. Lett. **118**(21), 211101 (2021).
26. M. Martì-Sabaté and D. Torrent, "Dipolar Localization of Waves in Twisted Photonic Crystal Plates," Phys. Rev. Appl. **15**(1), L011001 (2021).
27. W. Wang, W. Gao, X. Chen, F. Shi, G. Li, J. Dong, Y. Xiang, and S. Zhang, "Moiré Fringe Induced Gauge Field in Photonics," Phys. Rev. Lett. **125**(20), 203901 (2020).
28. K. Dong, T. Zhang, J. Li, Q. Wang, F. Yang, Y. Rho, D. Wang, C. P. Grigoropoulos, J. Wu, and J. Yao, "Flao Bands in Magic-Angle Bilayer Photonic Crystals at Small Twists," Phys. Rev. Lett. **126**(22), 223601 (2021).
29. T. Schwartz, G. Bartal, S. Fishman, and M. Segev, "Transport and Anderson localization in disordered two-dimensional photonic lattices," Nature **446**(7131), 52–55 (2007).
30. Y. Zong, S. Xia, L. Tang, D. Song, Y. Hu, Y. Pei, J. Su, Y. Li, and Z. Chen, "Observation of localized flat-band states in Kagome photonic lattices," Opt. Express **24**(8), 8877–8885 (2016).
31. B. A. Malomed, A. A. Nepomnyashchii, and M. I. Tribelskii, "Two-dimensional quasiperiodic structures in nonequilibrium systems," Sov. Phys. JETP **69**(2), 388–396 (1989).
32. L. D. Carr, M. J. Holland, and B. A. Malomed, "Macroscopic quantum tunning of Bose-Einstein condensates in a finite potential well," J. Phys. B: At., Mol. Opt. Phys. **38**(17), 3217–3231 (2005).
33. U. Peschel, T. Pertsch, and F. Lederer, "Optical Bloch oscillations in waveguide arrays," Opt. Lett. **23**(21), 1701–1703 (1998).
34. R. Morandotti, U. Peschel, J. S. Aitchison, H. S. Eisenberg, and Y. Silberberg, "Experimental Observation of Linear and Nonlinear Optical Bloch Oscillations," Phys. Rev. Lett. **83**(23), 4756–4759 (1999).
35. R. Iyer, J. S. Aitchison, J. Wan, M. M. Dignam, and C. M. de Sterke, "Exact dynamic localization in curved AlGaAs optical waveguide arrays," Opt. Express **15**(6), 3212–3223 (2007).
36. M. Ornigotti, G. D. Valle, D. Gatti, and S. Longhi, "Topological suppression of optical tunneling in a twisted annular fiber," Phys. Rev. A **76**(2), 023833 (2007).
37. L. Allen, M. W. Beijersbergen, R. J. C. Spreeuw, and J. P. Woerdman, "Orbital angular momentum of light and the transformation of Laguerre-Gaussian Laser modes," Phys. Rev. A **45**(11), 8185–8189 (1992).
38. Y. Shen, X. Wang, Z. Xie, C. Min, X. Fu, Q. Liu, M. Gong, and X. Yuan, "Optical vortices 30 years on: OAM manipulation from topological charge to multiple singularities," Light: Sci. Appl. **8**(1), 90 (2019).
39. K. Alnasser, S. Kamau, N. Hurley, J. Cui, and Y. Lin, "Resonance modes in moiré photonic patterns for twistoptics," OSA Continuum **4**(4), 1339–1347 (2021).
40. G. Roati, C. D'Errico, L. Fallani, M. Fattori, C. Fort, M. Zaccanti, G. Modugno, M. Modugno, and M. Inguscio, "Anderson localization of a non-interacting Bose-Einstein condensate," Nature **453**(7197), 895–898 (2008).
41. M. Modugno, "Exponential localization in one-dimensional quasi-periodic optical lattices," New J. Phys. **11**(3), 033023 (2009).
42. L. Levi, M. Rechtsman, B. Freedman, T. Schwartz, O. Manela, and M. Segev, "Disorder-Enhanced Transport in Photonic Quasicrystals," Science **332**(6037), 1541–1544 (2011).
43. E. A. Ostrovskaya and Y. S. Kivshar, "Photonic crystals for matter waves: Bose-Einstein condensates in optical lattices," Opt. Express **12**(1), 19–29 (2004).